Commun. Comput. Phys.
doi: 10.4208/cicp.120313.020813a

Vol. **15**, No. 3, pp. 692-711
March 2014

Novel Conservative Methods for Schrödinger Equations with Variable Coefficients over Long Time

Xu Qian[1,2,*], Yaming Chen[1,3] and Songhe Song[1]

[1] *Department of Mathematics and Systems Science, and State Key Laboratory of High Performance Computing, National University of Defense Technology, Changsha 410073, P.R. China.*
[2] *Program in Applied and Computational Mathematics, Princeton University, Princeton, NJ 08544, USA.*
[3] *School of Mathematical Sciences, Queen Mary University of London, London E1 4NS, UK.*

Received 12 March 2013; Accepted (in revised version) 2 August 2013

Available online 1 November 2013

Abstract. In this paper, we propose a wavelet collocation splitting (WCS) method, and a Fourier pseudospectral splitting (FPSS) method as comparison, for solving one-dimensional and two-dimensional Schrödinger equations with variable coefficients in quantum mechanics. The two methods can preserve the intrinsic properties of original problems as much as possible. The splitting technique increases the computational efficiency. Meanwhile, the error estimation and some conservative properties are investigated. It is proved to preserve the charge conservation exactly. The global energy and momentum conservation laws can be preserved under several conditions. Numerical experiments are conducted during long time computations to show the performances of the proposed methods and verify the theoretical analysis.

AMS subject classifications: 37M05, 65M70, 65T60

Key words: Schrödinger equation, wavelet collocation method, splitting technique, conservative property.

1 Introduction

The Schrödinger equations are very important in many branches of physics and applied mathematics, such as nonlinear quantum field theory, condensed matter, nonlinear optics, hydrodynamics, self-focusing in laser pulse, thermodynamic process in meso

*Corresponding author. *Email addresses:* xq@princeton.edu (X. Qian), yaming.chen@qmul.ac.uk (Y. M. Chen), shsong@nudt.edu.cn (S. H. Song)

scale systems, plasma and so on [1–7]. Meanwhile, most of real physical equations possess variable coefficient. For example, the dispersion-managed optical fibers and soliton lasers, certain inhomogeneous optical fibers, arterial mechanics, Laser-atom interaction and so on [8–13].

In this paper, firstly we consider the one-dimensional nonlinear Schrödinger (1D-NLS) equation with variable coefficients:

$$i\psi_t+\alpha(t)\psi_{xx}+v(x)\psi+\beta(t)|\psi|^2\psi=0, \tag{1.1a}$$

$$\psi(x,0)=\varphi(x), \tag{1.1b}$$

where $\alpha(t)$, $v(x)$ and $\beta(t)$ are bounded real functions, $\psi(x,t)$ is the complex-valued wave function, and $\alpha(t)$ is related to the second order dispersion coefficient. As usual, $i=\sqrt{-1}$, and $\varphi(x)$ is a smooth function such that

$$E_1(\varphi)=\int_{\mathbb{R}}|\varphi(x)|^2dx<+\infty, \tag{1.2}$$

(the so-called L_2-function). The 1D-NLS system admits following conservation laws

Proposition 1.1. The solution ψ of Eq. (1.1) satisfies:

(1) Global charge conservation:

$$\mathcal{Q}(\psi)=\int_{\mathbb{R}}|\varphi|^2dx=\mathcal{Q}(\varphi); \tag{1.3}$$

(2) Global momentum conservation:

$$\mathcal{M}(\psi)=\int_{\mathbb{R}}(\Re(\psi)\Im(\psi_x)-\Re(\psi_x)\Im(\psi))dx=\mathcal{M}(\varphi), \tag{1.4}$$

where $\Re$ and $\Im$ stand for the real part and the imaginary part, respectively;

(3) Global energy conservation: if $\alpha(t)$ and $\beta(t)$ are independent of t (i.e. $\alpha(t)=\alpha$, $\beta(t)=\beta$), then

$$\begin{aligned}\mathcal{E}(\psi)&=\int_{\mathbb{R}}\Big(\alpha|\psi_x|^2-v(x)|\psi|^2-\frac{\beta}{2}|\psi|^4\Big)dx\\&=\int_{\mathbb{R}}\Big(\alpha|\varphi_x|^2-v(x)|\varphi|^2-\frac{\beta}{2}|\varphi|^4\Big)dx=\mathcal{E}(\varphi).\end{aligned} \tag{1.5}$$

We will consider the following equations from the general form of Eq. (1.1):

(1) Cubic 1D-NLS equation

$$i\psi_t+\alpha(t)\psi_{xx}+\beta(t)|\psi|^2\psi=0. \tag{1.6}$$

The theoretical investigation of Eq. (1.6) can be found in [4] and references therein. We assume the solution ψ exists globally and satisfies $\lim_{|x|\to+\infty}(|\psi|+|\psi_x|)=0$.

(2) Gross-Pitaevskii (GP) equation

$$i\psi_t+\alpha\psi_{xx}+v(x)\psi+\beta|\psi|^2\psi=0. \tag{1.7}$$

For this case, we assume the solution of ψ satisfies $\lim_{|x|\to+\infty}(|\psi|+|\psi_{xx}|)=0$.

Meanwhile, we consider a two-dimensional linear Schrödinger (2D-LS) equation of one atom in an intense laser field [14]

$$i\psi_t+\frac{1}{2}\psi_{xx}+\frac{1}{2}\psi_{yy}+(v(x,y)-\varepsilon(t)x)\psi=0, \tag{1.8}$$

where $\psi(x,y,t)$ is the wave function, $v(x,y)$ is the long range potential and $\varepsilon(t)$ is the external laser field.

Since available theoretical solutions for Schrödinger equations are limited, investigating numerically is an important tool to understand physical behavior of the system. There are many numerical methods for Schrödinger equations. Delfour et al. [15] proposed general finite difference method. Meng et al. [16] proposed an orthogonal spline collocation method. Chang et al. [17] discussed several different schemes such as Crank-Nicolson, Hospscotch scheme, split-step Fourier scheme, pseudo-spectral scheme for generalized NLS equation. Bao et al. [5, 7] proposed a time-splitting Laguerre-Hermite pseudo-spectral method and a Fourier spectral method for Gross-Pitaevskii equation. Compact finite difference schemes for one-dimensional case are constructed in [18, 19]. In addition, numerous symplectic and multi-symplectic methods have been constructed to simulate Schrödinger system and other Hamiltonian equations due to their long time simulation property and good preservation property of conservative quantities of original problem. Chen et al. [20,21] proposed several symplectic and multi-symplectic methods for NLS equations. The multi-symplectic Runge-Kutta and Fourier spectral methods were employed to solve the fourth-order Schrödinger equations with trapped term by Hong et al. in [22]. Chen et al. [23, 24] took the splitting technique into the multi-symplectic integrator and Cai et al. [25] proposed some local structure-preserving algorithms for solving coupled NLS equation. But the above methods are almost to solve Schrödinger equations with constant coefficients or one-dimensional cases. Hong et al. [26] constructed a multi-symplectic scheme for Schrödinger equations with some special variable coefficients. For the system with variable coefficients, the common way is to modify the finite difference methods to cope with the general cases. Sometimes, it is difficult for the finite difference methods to meet requirements of high accuracy and high resolution of complex physical process. Symplectic, multi-symplectic and other structure-preserving methods can preserve the intrinsic properties of original problems and conservation laws during long time simulations. Theoretically, all most real physical process with negligible dissipation can be cast in suitable Hamiltonian formulation in phase space with symplectic structure, which means the symplectic-preserving algorithms can hold this properties naturally. But in practice, the structure-preserving methods have their own constrains. Firstly, most of symplectic and multi-symplectic methods are constructed with suitable boundary conditions, such as periodic or homogeneous boundary

conditions. Secondly, it is very hard to propose symplectic and multi-symplectic formulism for many complex systems. In addition, although it exists some methods to write Hamiltonian equation as multi-symplectic form [27, 28], there are still many unsolved problems, which make the construction of multi-symplectic form for a given PDE a bit complicated [29].

Our main aim is to construct efficient and conservative algorithms for 1D-NLS equation and 2D-LS equation with variable coefficient without considerations of symplectic or multi-symplectic conservation formulations. In this paper, we propose the WCS method, and the analogous FPSS method as comparison. The Schrödinger system is split into two subsystems. One can be solved exactly. For the other, wavelet collocation method [30] and Fourier pseudospectral method [23] are employed in spatial discretization, respectively. Wavelet collocation method makes the corresponding spatial differentiation matrix sparse and demands less computations. Fourier pseudospectral method has high accuracy, and does not need transformation between the Fourier space and physical space. So it is also efficient in computations. For the WCS method, the convergence property is discussed. It is proved to preserve the charge conservation exactly. The global energy and momentum conservation laws also can be preserved under several conditions.

The paper is organized in the following way. In Section 2, the splitting technique for Schrödinger equation is introduced. In Section 3, the WCS method formulations for 1D and 2D cases are proposed. In Section 4, some theoretical analysis, such as convergence and conservative properties, are presented. The analogous FPSS method and numerical experiments are presented in Section 5, which show the effectiveness of the proposed algorithms. Finally, conclusions are made in Section 6.

2 Splitting technique for Schrödinger equation

In this section, we mainly describe the splitting technique for 1D-NLS equation briefly. The basic idea of splitting technique for the nonlinear equations is to decompose a system into linear and nonlinear subsystems on each time step.

$$w_t = (\mathcal{L}(t)+\mathcal{N}(t,w))w, \tag{2.1}$$

where $\mathcal{L}$ and $\mathcal{N}$ are linear and nonlinear operators, respectively. We decompose the nonlinear system into the following subsystems:

$$w_t = \mathcal{L}(t)w, \tag{2.2a}$$

$$w_t = \mathcal{N}(t,w)w. \tag{2.2b}$$

Now, based on the Strang's splitting idea [31, 32] to solve (2.2a)-(2.2b) over $t \in [t_n, t_{n+1}]$, we have the following:

$$w^* = \exp\Big[\frac{1}{2}\int_{t_n}^{t_{n+1}} \mathcal{N}(t,w(t_n))dt\Big] w(t_n), \tag{2.3a}$$

$$w^{**}=\exp\Big[\int_{t_n}^{t_{n+1}}\mathcal{L}(t)dt\Big]w^{*}, \tag{2.3b}$$

$$w(t_{n+1})=\exp\Big[\frac{1}{2}\int_{t_n}^{t_{n+1}}\mathcal{N}(t,w^{**})dt\Big]w^{**}. \tag{2.3c}$$

In this method, we split Eq. (1.1) into linear equation,

$$\mathcal{L}:\ \psi_t=i\alpha(t)\psi_{xx}, \tag{2.4}$$

and nonlinear equation

$$\mathcal{N}:\ \psi_t=iv(x)\psi+i\beta(t)|\psi|^2\psi. \tag{2.5}$$

This is the second-order version of the Strang splitting technique. In fact, we can construct arbitrary order for the splitting technique. After time-splitting, the nonlinear subsystem (2.5) can be solved exactly, while the linear subsystem (2.4) could be solved by using wavelet collocation method and Fourier pseudospectral method in space, respectively. In the following section, we will give the detailed algorithms of the WCS method for 1D and 2D cases.

3 Wavelet collocation splitting method

In this section, a wavelet collocation method [30, 33], which is based on the autocorrelation function of Daubechies scaling function of order M, is used for space discretization. Then, we demonstrate the formulation of the WCS method for one-dimensional and two-dimensional cases.

3.1 One-dimensional case

Consider the periodic boundary condition $\psi(a,t)=\psi(b,t)$, where a and b are integers. For a fixed scale $J=constant$, the differential operator $\frac{\partial^k}{\partial x^k}$ yields a wavelet collocation differential matrix B_k, which can be expressed as

$$(B_k)_{m,n}=\begin{cases}2^{kJ}\theta^{(k)}(m-n), & m-(M-1)\le n\le m+(M-1);\\ 2^{kJ}\theta^{(k)}(-i), & m-n=N-i,\ 1\le i\le M-1;\\ 2^{kJ}\theta^{(k)}(i), & n-m=N-i,\ 1\le i\le M-1;\\ 0, & \text{otherwise.}\end{cases} \tag{3.1}$$

Here $N=2^J(b-a)$ is the grid number. There is no analytical expression for $\theta^{(k)}(x)$ $(k=0,1,2,\cdots)$, but we can get the numerical values of the function $\theta^{(k)}(x)$ at integer point $x=i$ $(i=0,\pm1,\cdots,\pm(M-1))$. From the properties of B_k, we can notice that B_{2k} is symmetric and B_{2k+1} is skew-symmetric.

Now, we approximate the space derivative in Eq. (2.4) by using the wavelet collocation method

$$\frac{\partial}{\partial t}\psi_j = i\alpha(t)(B_2\Psi)_j, \tag{3.2}$$

where $\Psi=(\psi_0,\psi_1,\cdots,\psi_{N-1})^{\mathrm{T}}$, $j=0,1,\cdots,N-1$.

Then, we apply Euler mid-point method to solve above subsystem in time direction

$$\psi_j^{n+1}=\psi_j^n+\frac{i\tau}{2}(\alpha^{n+1}+\alpha^n)(B_2\Psi^{n+1/2})_j, \tag{3.3}$$

where $\Psi^{n+1/2}=(\Psi^{n+1}+\Psi^n)/2$, and τ is time-step.

By letting $\psi=p+iq$, the system (3.3) is equivalent to

$$p_j^{n+1}=p_j^n-\frac{\tau}{4}(\alpha^{n+1}+\alpha^n)[B_2(Q^{n+1}+Q^n)]_j, \tag{3.4a}$$

$$q_j^{n+1}=q_j^n+\frac{\tau}{4}(\alpha^{n+1}+\alpha^n)[B_2(P^{n+1}+P^n)]_j, \tag{3.4b}$$

where $P^n=(p_0^n,p_1^n,\cdots,p_{N-1}^n)^{\mathrm{T}}$, $Q^n=(q_0^n,q_1^n,\cdots,q_{N-1}^n)^{\mathrm{T}}$.

We obtain the following algorithm of WCS method for Eq. (1.1):

$$\psi_j^*=\exp\left[i\left(v(x_j)+|\psi_j^n|^2\int_{t_n}^{t_{n+1}}\beta(t)dt\right)/2\right]\psi_j^n, \qquad j=0,1,\cdots,N-1, \tag{3.5a}$$

$$\psi_j^{**}=\psi_j^*+\frac{i\tau}{4}(\alpha^{n+1}+\alpha^n)(B_2(\Psi^{**}+\Psi^*))_j, \qquad j=1,2,\cdots,N-2, \tag{3.5b}$$

$$\psi_0^{**}=\psi_{N-1}^{**}=0, \tag{3.5c}$$

$$\psi_j^{n+1}=\exp\left[i\left(v(x_j)+|\psi_j^{**}|^2\int_{t_n}^{t_{n+1}}\beta(t)dt\right)/2\right]\psi_j^{**}, \qquad j=0,1,\cdots,N-1. \tag{3.5d}$$

3.2 Two-dimensional case

According to the splitting technique, We can split the 2D-LS equation (1.8) into two subsystems:

$$\mathcal{L}_1:\ \psi_t=i\left(\frac{1}{2}\psi_{xx}+\frac{1}{2}\psi_{yy}\right), \tag{3.6a}$$

$$\mathcal{L}_2:\ \psi_t=i(v(x,y)-\varepsilon(t)x)\psi. \tag{3.6b}$$

After time-splitting, the subsystem (3.6b) can be solved exactly, while the subsystem (3.6a) could be solved by using two-dimensional wavelet collocation method in space.

By letting $\psi=p+iq$, the subsystem (3.6a) is equivalent to

$$p_t=-\left(\frac{1}{2}q_{xx}+\frac{1}{2}q_{yy}\right), \tag{3.7a}$$

$$q_t=\frac{1}{2}p_{xx}+\frac{1}{2}p_{yy}. \tag{3.7b}$$

Consider the subsystem (3.7) with periodic boundary conditions in $[0,L]\times[0,L]$, where L is an integer. We also use the wavelet collocation method to approximate $p(x,y,t)$, $q(x,y,t)$, and obtain the wavelet collocation semi-discretization for the 2D-LS equation

$$\frac{\partial}{\partial t}p_{l,l'}=-\frac{1}{2}(AQ)_{l,l'}, \tag{3.8a}$$

$$\frac{\partial}{\partial t}q_{l,l'}=\frac{1}{2}(AP)_{l,l'}, \tag{3.8b}$$

where $P=(p_{0,0},\cdots,p_{N-1,0},p_{0,1},\cdots,p_{N-1,1},\cdots,p_{0,N-1},\cdots,p_{N-1,N-1})^{\mathrm{T}}$, $Q=(q_{0,0},\cdots,q_{N-1,0},q_{0,1},\cdots,q_{N-1,1},\cdots,q_{0,N-1},\cdots,q_{N-1,N-1})^{\mathrm{T}}$, $l,l'=0,1,\cdots,N-1$, $N=L\cdot 2^J$, J is the fixed scale, $A=B_2\otimes I_N+I_N\otimes B_2$, $\otimes$ is Kronecker inner product, I_N is the $N\times N$ identity matrix, B_k is the $N\times N$ circulant matrix, which has the same definition in (3.1).

We also use mid-point method to solve above subsystem in time direction

$$P^{n+1}=P^n-\frac{\tau}{2}(AQ^{n+1/2}), \tag{3.9a}$$

$$Q^{n+1}=Q^n+\frac{\tau}{2}(AP^{n+1/2}), \tag{3.9b}$$

where $P^{n+1/2}=(P^{n+1}+P^n)/2$, $Q^{n+1/2}=(Q^{n+1}+Q^n)/2$, and τ is time-step. It can also be rewritten as

$$\psi_{l,l'}^{n+1}=\psi_{l,l'}^n+\frac{i\tau}{2}(A\Psi^{n+1/2})_{l,l'}. \tag{3.10}$$

We can obtain the algorithm of WCS method for the 2D-LS equation (1.8):

$$\psi_{l,l'}^{*}=\exp\left[i\left(v(x_l,y_{l'})\tau-x_l\int_{t_n}^{t_{n+1}}\varepsilon(t)dt\right)/2\right]\psi_{l,l'}^n,\quad l,l'=0,1,\cdots,N-1, \tag{3.11a}$$

$$\psi_{l,l'}^{**}=\psi_{l,l'}^{*}+\frac{i\tau}{4}(A(\Psi^{**}+\Psi^{*}))_{l,l'},\qquad l,l'=1,2,\cdots,N-2, \tag{3.11b}$$

$$\psi_{0,l'}^{**}=\psi_{N-1,l'}^{**}=\psi_{l,0}^{**}=\psi_{l,N-1}^{**}=0,\qquad l,l'=0,1,\cdots,N-1, \tag{3.11c}$$

$$\psi_{l,l'}^{n+1}=\exp\left[i\left(v(x_l,y_{l'})\tau-x_l\int_{t_n}^{t_{n+1}}\varepsilon(t)dt\right)/2\right]\psi_{l,l'}^{**},\quad l,l'=0,1,\cdots,N-1. \tag{3.11d}$$

4 Error estimation and conservative properties of the WCS method

In this section, we first present error estimate of the WCS method for 1D-NLS equation and prove the method is convergent. Second, we display some conservative properties. The analysis for two-dimensional case and the FPSS method has similar deductive procedure. For simplicity, we only demonstrate the proof of the WCS method for one-dimensional case.

Lemma 4.1. [34] *Let $0\le r\le s\le 2M-1$, $s\ge 1$, and $u\in H^s(R)$, then*

$$\|u-I_Ju\|_r\le C2^{-J(s-r)}\|u\|_s, \tag{4.1}$$

where $\|\cdot\|_r$ and $\|\cdot\|_s$ denote the norm of Sobolev space $H^r(R)$ and $H^s(R)$, respectively. I is the interpolation operator $I_Ju(x)=2^{-\frac{J}{2}}\sum_k u(2^{-J}k)\theta_{J,k}(x)$.

Since the numerical solver for the nonlinear subproblem (2.5) is exact, the error is bound up with linear subproblem.

Theorem 4.1. *Suppose $p(x,t)$, $q(x,t)\in H^s(a,b)$, $s\ge\frac{5}{2}$, $\forall t\in[0,T]$, $p(x,t)$, $q(x,t)\in C^4(a,b)$, $\alpha(t)\equiv\alpha$. Then the truncation error R^n of the wavelet collocation method* (3.3) *satisfies*

$$\|R^n\|\le\mathcal{O}(\tau+2^{-J(s-2)}).$$

Proof. Let $\Psi^n=(\psi(x_{a\cdot 2^J},t_n),\psi(x_{a\cdot 2^J+1},t_n),\cdots,\psi(x_{b\cdot 2^J-1},t_n))$ be the solution of (2.4). Based on Taylor expanding, the following equations can be obtained,

$$\begin{aligned}&\Psi^{n+1}-\Psi^n=\tau\Psi_t^n+\mathcal{O}(\tau^2),\\&\Psi^{n+1}+\Psi^n=2\Psi^n+\tau\Psi_t^n+\mathcal{O}(\tau^2).\end{aligned}$$

Hence, the truncation error of the wavelet collocation method (3.3) goes as

$$\begin{aligned}R^n&=\frac{\Psi^{n+1}-\Psi^n}{\tau}-i\alpha B_2\left(\frac{\Psi^{n+1}+\Psi^n}{2}\right)\\&=\Psi_t^n+\mathcal{O}(\tau)-i\alpha B_2\left(\Psi^n+\frac{1}{2}\tau\Psi_t^n+\mathcal{O}(\tau^2)\right)-(\Psi_t^n-i\alpha\Psi_{xx}^n)\\&=i\alpha(\Psi_{xx}^n-B_2\Psi^n)-\frac{i\tau}{2}\alpha B_2\Psi_t^n+\mathcal{O}(\tau).\end{aligned}$$

From Lemma 4.1, we get

$$\|\psi_{xx}^n-\theta_{xx}\psi^n\|_{L^2}\le\|\psi^n-I_J\psi^n\|_2\le C2^{-J(s-2)}\|\psi^n\|_s,$$

where $\|\cdot\|_s$ denotes the norm of Sobolev space $H^s(a,b)$. Notice that

$$\|\Psi_{xx}^n-B_2\Psi^n\|=\left\{\sum_{k=a\cdot 2^J}^{b\cdot 2^J-1}2^{-J}\cdot[\psi_{xx}^n(x_k)-\theta_{xx}\psi^n(x_k)]^2\right\}^{1/2}$$

is the rectangle quadrature rule approximation to $\|\psi_{xx}^n-\theta_{xx}\psi^n\|_{L^2}$. Therefore, the error estimate follows:

$$\begin{aligned}\|R^n\|&\le|\alpha|\cdot\|\Psi_{xx}^n-B_2\Psi^n\|+\tau\left\|\frac{1}{2}B_2\Psi_t^n\right\|+\mathcal{O}(\tau)\\&\le\mathcal{O}(2^{-J(s-2)}+\tau).\end{aligned}$$

The proof is complete. □

Then, the following error estimate is obtained.

Theorem 4.2. *Suppose $\psi(x,t)$ is the same as in Theorem 4.1, then the error estimate e^M of the wavelet collocation method* (2.4) *satisfies*

$$\|e^M\| \leq \mathcal{O}(\tau + 2^{-J(s-2)}).$$

Proof. Suppose Ψ^n and Ψ_J^n are the solutions of Eq. (2.4) and Eq. (3.3) respectively, and define the error at t_n as e^n, i.e.

$$e^n = \Psi^n - \Psi_J^n,$$

then

$$R^n = i\frac{e^{n+1}-e^n}{\tau} + \alpha B_2\Big(\frac{e^{n+1}+e^n}{2}\Big). \tag{4.2}$$

Define

$$\delta_t e^{n+1/2} = \frac{e^{n+1}-e^n}{\tau}, \quad e^{n+1/2} = \frac{e^{n+1}+e^n}{2},$$

and make inner product of the both sides of Eq. (4.2) with $2e^{n+1/2}$, it follows that

$$\langle R^n, 2e^{n+1/2}\rangle = i\langle \delta_t e^{n+1/2}, 2e^{n+1/2}\rangle + \langle \alpha B_2 e^{n+1/2}, 2e^{n+1/2}\rangle, \tag{4.3}$$

and we notice that B_2 is a real symmetric and negative semi-definite matrix [30], hence

$$\langle B_2 e^{n+1/2}, e^{n+1/2}\rangle \leq 0. \tag{4.4}$$

We take the imaginary part of Eq. (4.3)

$$\frac{1}{\tau}(\|e^{n+1}\|^2 - \|e^n\|^2) = \Im\langle R^n, 2e^{n+1/2}\rangle. \tag{4.5}$$

In addition,

$$|\Im\langle R^n, 2e^{n+1/2}\rangle| \leq \|R^n\|^2 + \|e^n\|^2 + \|e^{n+1}\|^2. \tag{4.6}$$

Therefore,

$$\|e^{n+1}\|^2 - \|e^n\|^2 \leq \tau(\|R^n\|^2 + \|e^n\|^2 + \|e^{n+1}\|^2). \tag{4.7}$$

We define a discrete function $W^n = \|e^n\|^2$, and rewrite (4.7)

$$W^{n+1} - W^n \leq \tau(A^n + W^n + W^{n+1}), \tag{4.8}$$

where $A^n = \|R^n\|^2$. And the estimate of W^M can be obtained by using Gronwall inequation [35],

$$W^M \leq \Big(W^0 + \tau\sum_{k=1}^{M} A^k\Big)e^{4T}, \quad M\tau = T. \tag{4.9}$$

Because

$$\|e^0\|^2 = \|R^0\|^2 = 0, \quad \|e^1\|^2 = \mathcal{O}(\tau + 2^{-J(s-2)})^2,$$

we have

$$W^0 = \mathcal{O}(\tau + 2^{-J(s-2)})^2.$$

In addition, from Theorem 4.1, we have

$$A^k = \|R^n\|^2 = \mathcal{O}(\tau + 2^{-J(s-2)})^2.$$

And based on the Gronwall inequation, it follows that

$$W^M = \|e^M\|^2 \leq C \cdot \mathcal{O}(\tau + 2^{-J(s-2)})^2.$$

Finally, we have obtained the error estimate as

$$\|e^M\| \leq \mathcal{O}(\tau + 2^{-J(s-2)}).$$

The proof is complete. □

Now, we discuss some conservative properties of proposed method.

Theorem 4.3. *The WCS method* (3.5) *preserves the charge*

$$\mathcal{Q}^{n+1} = \|\Psi^{n+1}\|^2 = \triangle x \sum_j |\psi^{n+1}|^2 = \cdots = \mathcal{Q}^0, \tag{4.10}$$

where $\triangle x$ *is the space step size.*

Proof. It is obviously revealed that the algorithm (3.5) for nonlinear subsystem is exact. Therefore, we have

$$\|\Psi^*\|^2 = \|\Psi^n\|^2, \quad \|\Psi^{n+1}\|^2 = \|\Psi^{**}\|^2. \tag{4.11}$$

Then, the nonlinear subsystem (3.3) can be rewritten as

$$i\frac{\Psi^{**} - \Psi^*}{\tau} + \frac{\alpha^{n+1} + \alpha^n}{4} B_2(\Psi^{**} + \Psi^*) = 0. \tag{4.12}$$

We make inner product of the both sides of (4.12) with $\Psi^{**} + \Psi^*$, it follows that

$$\frac{i}{\tau}(\|\Psi^{**}\|^2 - \|\Psi^*\|^2 + 2i\Im(\Psi^{**}\bar{\Psi}^*)) + \frac{\alpha^{n+1} + \alpha^n}{4}\langle B_2(\Psi^{**} + \Psi^*), (\Psi^{**} + \Psi^*)\rangle = 0. \tag{4.13}$$

The term $\langle B_2(\Psi^{**} + \Psi^*), (\Psi^{**} + \Psi^*)\rangle$ is real. Therefore, the imaginary part of Eq. (4.13) implies

$$\|\Psi^{**}\|^2 = \|\Psi^*\|^2. \tag{4.14}$$

Combining Eq. (4.11) with Eq. (4.14), we obtain

$$\|\Psi^{n+1}\|^2 = \|\Psi^n\|^2. \tag{4.15}$$

The proof is complete. □

Theorem 4.4. *If $\alpha(t)\equiv\alpha$, $\beta(t)\equiv\beta$, and the wave function ψ is separable, i.e.*

$$\psi(x,t)=X(x)T(t), \tag{4.16}$$

the WCS method (3.5) *satisfies the discrete global energy conservation law*

$$\begin{aligned}&\triangle x\sum_j\Big(\alpha|(B_2\Psi^{n+1})_j|^2-v_j|\psi_j^{n+1}|^2-\frac{\beta}{2}|\psi_j^{n+1}|^4\Big)\\=&\triangle x\sum_j\Big(\alpha|(B_2\Psi^{n})_j|^2-v_j|\psi_j^{n}|^2-\frac{\beta}{2}|\psi_j^{n}|^4\Big).\end{aligned} \tag{4.17}$$

In other words

$$\mathcal{E}^{n+1}=\mathcal{E}^n=\cdots=\mathcal{E}^0. \tag{4.18}$$

Proof. According to (4.10) and (4.16), we have

$$|T^{n+1}|^2=|T^n|^2. \tag{4.19}$$

Then,

$$\begin{aligned}&\triangle x\sum_j\Big(\alpha|(B_2\Psi^{n+1})_j|^2-v_j|\psi_j^{n+1}|^2-\frac{\beta}{2}|\psi_j^{n+1}|^4\Big)\\=&\triangle x\sum_j\Big(\alpha|T^{n+1}|^2|(B_2X)_j|^2-v_j|T^{n+1}|^2|X_j|^2-\frac{\beta}{2}|T^{n+1}|^4|X_j|^4\Big)\\=&\triangle x\sum_j\Big(\alpha|T^{n}|^2|(B_2X)_j|^2-v_j|T^{n}|^2|X_j|^2-\frac{\beta}{2}|T^{n}|^4|X_j|^4\Big)\\=&\triangle x\sum_j\Big(\alpha|(B_2\Psi^{n})_j|^2-v_j|\psi_j^{n}|^2-\frac{\beta}{2}|\psi_j^{n}|^4\Big).\end{aligned} \tag{4.20}$$

Thus, Theorem 4.4 is proved. □

The discrete global momentum conservation law below has similar proof.

Theorem 4.5. *Let the conditions of Theorem* 4.4 *be satisfied. the WCS method* (3.5) *satisfies the discrete global momentum conservation law*

$$\begin{aligned}&\triangle x\sum_j\Big(\Re(\psi_j^{n+1})\Im((B_2\Psi^{n+1})_j)-\Re((B_2\Psi^{n+1})_j)\Im(\psi_j^{n+1})\Big)\\=&\triangle x\sum_j\Big(\Re(\psi_j^{n})\Im((B_2\Psi^{n})_j)-\Re((B_2\Psi^{n})_j)\Im(\psi_j^{n})\Big).\end{aligned} \tag{4.21}$$

In other words

$$\mathcal{M}^{n+1}=\mathcal{M}^n=\cdots=\mathcal{M}^0. \tag{4.22}$$

5 Numerical experiments

In the section, we conduct some typical numerical examples to show the effectiveness and high accuracy for proposed algorithms during long time simulations. The results are compared with Fourier pseudospectral splitting method. In brief, we use Fourier spectral differential matrix in spatial discretization.

For the one-dimensional case, the first-order differential operator ∂_x yields the Fourier spectral differential matrix D_1. Here, D_1 is an $N\times N$ skew-symmetric matrix whose elements are

$$(D_1)_{j,s}=\begin{cases}\dfrac{1}{2}(-1)^{j+s}\mu\cot\Big(\mu\dfrac{x_j-x_s}{2}\Big), & s\neq j,\\ 0, & s=j,\end{cases}$$

for $j,s=1,2,\cdots,N$, and $\mu=2\pi/L$. The second-order Fourier spectral differential matrix is defined as $D_2=D_1^2$. For 1D-NLS equation, the wavelet collocation differential matrix B_2, which is displayed in the discrete scheme (3.3), discrete global energy (4.17), and discrete global momentum (4.21), is substituted by the second-order Fourier spectral differential matrix D_2. Since D_2 is symmetric matrix, the FPSS method has the similar conservative properties. On the analogy of FPSS in 1D-NLS equation, we have the similar changes for 2D-LS equation likewise. For more details, one can consult [23,36] and references therein.

In addition, the autocorrelation function AD30 is used for wavelet collocation method in the following examples. We solve the implicit parts of our algorithms by using the fixed-point iteration with tolerance $\varepsilon=10^{-15}$.

Example 5.1. We consider the 1D-NLS equation (1.1) with $v(x)=0$ in following two cases:

(a) Periodic case:

$$\alpha(t)=\frac{1}{2}\cos(t),\quad \beta(t)=\frac{\cos(t)}{\sin(t)+3};$$

(b) Quasi-periodic case:

$$\alpha(t)=\frac{1}{2}(\cos(t)+\sqrt{2}\cos(\sqrt{2}t)),\quad \beta(t)=\frac{\cos(t)+\sqrt{2}\cos(\sqrt{2}t)}{\sin(t)+\sin(\sqrt{2}t)+5}.$$

Based on the results in [13], the problem (a) has a periodic solitary-wave solution

$$\psi(x,t)=\frac{1}{\sqrt{\sin(t)+3}}\mathrm{sech}\Big(\frac{x}{\sin(t)+3}\Big)\exp\Big(\frac{i(x^2-1)}{2(\sin(t)+3)}\Big),$$

and the problem (b) has a quasi-periodic solitary-wave solution

$$\psi(x,t)=\frac{1}{\sqrt{\sin(t)+\sin(\sqrt{2}t)+5}}\mathrm{sech}\Big(\frac{x}{\sin(t)+\sin(\sqrt{2}t)+5}\Big)\times\exp\Big(\frac{i(x^2-1)}{2(\sin(t)+\sin(\sqrt{2}t)+5)}\Big).$$

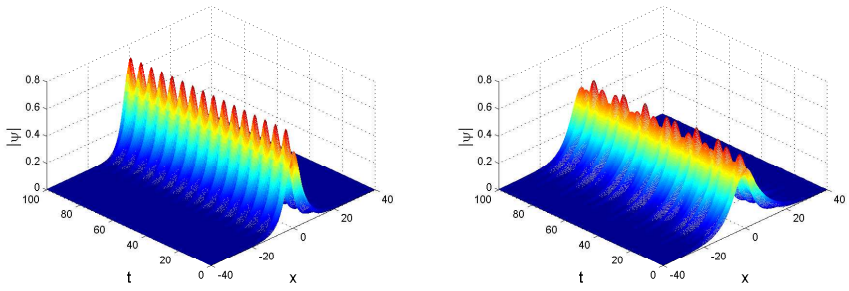

Figure 1: The periodic (left) and quasi-periodic (right) solitary waves by WCS method ($\tau=0.005$, $\Delta x=0.5$).

For this example, we mainly verify the numerical behaviors of the two methods during long time computations. In Fig. 1, the periodic and quasi-periodic solitary waves are pictured numerically by WCS method till time $t=100$, respectively. The L^∞ and L^2 errors of the two problems by the WCS and FPSS are displayed in Tables 1 and 2. The discrete

Table 1: Comparison of errors at different time with the two algorithms in Example 5.1(a) ($\tau=0.005$, $\Delta x=0.5$).

Time	Real part		Imaginary part	
	L^∞ error	L^2 error	L^∞error	L^2 error
WCS method				
5	1.240E-4	3.258E-4	1.245E-4	3.133E-4
10	3.199E-4	7.901E-4	3.030E-4	7.740E-4
20	8.007E-5	2.587E-4	7.438E-5	2.653E-4
30	1.477E-4	3.574E-4	1.477E-4	3.853E-4
40	2.315E-4	6.804E-4	2.293E-4	7.033E-4
50	8.374E-5	1.575E-4	1.548E-4	2.764E-4
60	2.965E-4	8.034E-4	2.947E-4	8.406E-4
70	9.463E-5	2.434E-4	1.730E-4	3.819E-4
80	1.939E-4	4.487E-4	3.313E-4	4.487E-4
90	1.823E-4	6.050E-4	2.085E-4	7.029E-4
100	1.647E-4	2.780E-4	3.302E-4	5.273E-4
FPSS method				
5	2.327E-4	7.969E-4	1.817E-4	6.760E-4
10	3.319E-4	1.019E-3	3.543E-4	1.058E-3
20	1.772E-4	6.538E-4	2.000E-4	8.120E-4
30	2.046E-4	7.834E-4	1.799E-4	6.818E-4
40	2.812E-4	8.826E-4	2.318E-4	8.559E-4
50	1.691E-4	6.625E-4	1.685E-4	5.499E-4
60	3.483E-4	9.649E-4	3.072E-4	9.912E-4
70	2.056E-4	6.425E-4	1.697E-4	6.540E-4
80	2.153E-4	8.166E-4	3.190E-4	8.279E-4
90	2.328E-4	8.779E-4	2.594E-4	1.012E-3
100	2.227E-4	6.024E-4	3.724E-4	9.347E-4

Table 2: Comparison of errors at different time with the two algorithms in Example 5.1(b) ($\tau=0.005$, $\Delta x=0.5$).

Time	Real part		Imaginary part	
	L^∞ error	L^2 error	L^∞error	L^2 error
WCS method				
5	1.373E-4	4.821E-4	1.341E-4	4.791E-4
10	3.688E-4	1.371E-3	3.600E-4	1.371E-3
20	3.561E-4	1.438E-3	3.636E-4	1.428E-3
30	3.484E-4	9.882E-4	3.335E-4	9.815E-4
40	1.866E-4	7.050E-4	1.823E-4	6.955E-4
50	1.684E-4	6.210E-4	1.647E-4	6.258E-4
60	5.608E-4	2.006E-3	5.762E-4	2.005E-3
70	2.051E-4	7.085E-4	2.032E-4	7.319E-4
80	1.390E-4	4.675E-4	1.471E-4	5.263E-4
90	2.897E-4	1.236E-3	2.909E-4	1.257E-3
100	3.673E-4	1.218E-3	3.741E-4	1.245E-3
FPSS method				
5	1.768E-4	8.018E-4	1.970E-4	7.164E-4
10	3.952E-4	1.543E-3	3.617E-4	1.410E-3
20	3.831E-4	1.565E-3	4.271E-4	1.583E-3
30	3.301E-4	1.110E-3	4.041E-4	1.278E-3
40	1.743E-4	8.379E-4	2.038E-4	9.110E-4
50	1.602E-4	7.836E-4	1.691E-4	8.238E-4
60	5.536E-4	2.058E-3	5.412E-4	2.075E-3
70	2.368E-4	9.498E-4	2.525E-4	9.387E-4
80	2.106E-4	8.492E-4	2.646E-4	8.201E-4
90	3.212E-4	1.224E-3	3.484E-4	1.270E-3
100	3.789E-4	1.376E-3	4.064E-4	1.438E-3

charge errors are showed in Fig. 2 and Fig. 3.

For the periodic problem, the numerical results indicate that the WCS and FPSS can simulate the periodic solitary wave exactly and preserve discrete charge conservation law well. The discrete charge conservation laws by the two methods are preserved to an accuracy 10^{-14}. The errors, in some sense, of WCS method seems a little less than FPSS method. For the quasi-periodic problem, the two methods have the similar errors during the period of computations. The charge preserving by FPSS method seems better than that by WCS method.

Numerical results of both two problems show the trends of errors do not increase obviously when t becomes larger, and the discrete charge errors are also stable.

Example 5.2. For Gross-Pitaevskii equation, we consider Eq. (1.1) with the parameters $\alpha(t)=\frac{1}{2}$, $\beta(t)=-1$, $v(x)=-\cos^2(x)$. Based on the results in [21], this problem has the exact solution

$$\psi(x,t)=\sin(x)\exp(-i3t/2).$$

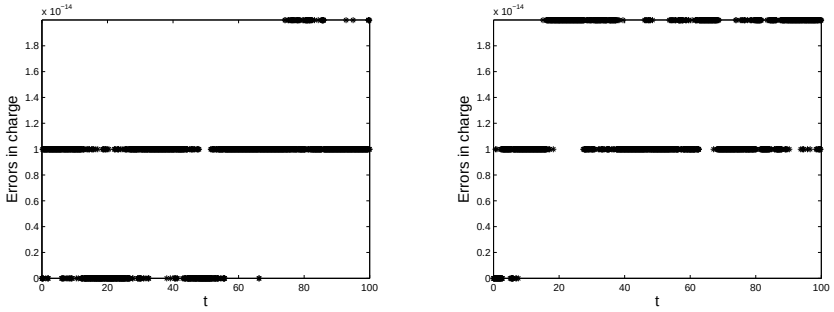

Figure 2: Comparison of the discrete charge conservation errors for Example 5.1(a) by WCS method (left) and FPSS method (right).

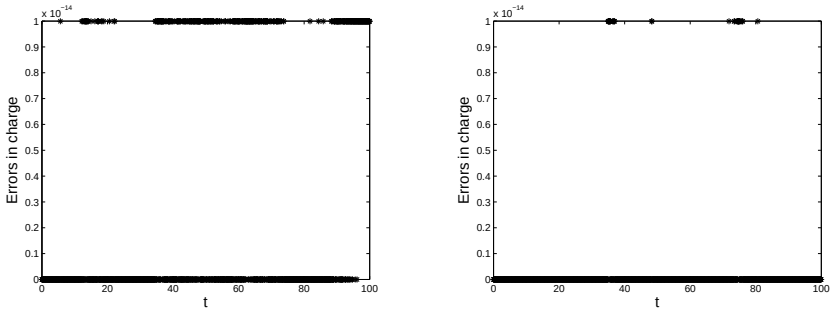

Figure 3: Comparison of the discrete charge conservation errors for Example 5.1(b) by WCS method (left) and FPSS method (right).

We solve the problem by both WCS and FPSS method with the periodic boundary condition in $[0,2\pi]$. For the WCS method, we take a coordinate transform $x=2\pi\xi$, and the boundary condition is equivalent to $[0,1]$. The L^∞ and L^2 errors are contained in Table 3. The errors of WCS method are a little less than the FPSS method. The global energy and charge errors are showed in Figs. 4 and 5. We can see both WCS and FPSS method

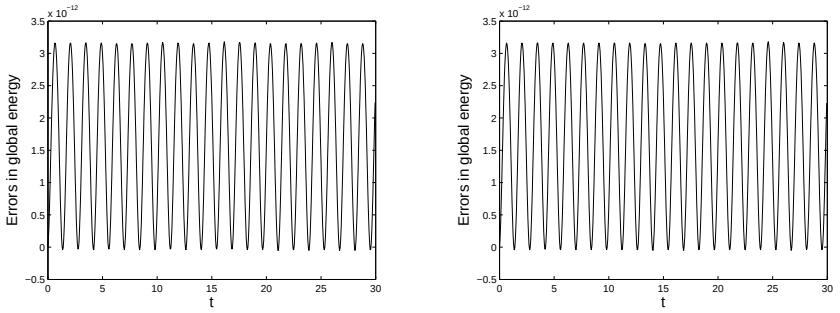

Figure 4: Comparison of the discrete global energy conservation errors for Example 5.2 by WCS method (left) and FPSS method (right).

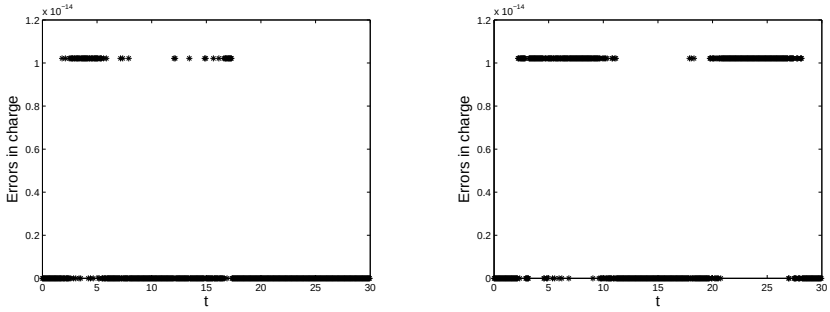

Figure 5: Comparison of the discrete charge conservation errors for Example 5.2 by WCS method (left) and FPSS method (right).

Table 3: Comparison of errors at different time with the two algorithms in Example 2 ($\tau=0.005$, $\Delta x=2\pi/64$).

Time	Real part		Imaginary part	
	L^∞ error	L^2 error	L^∞error	L^2 error
WCS method				
5	3.599E-7	6.362E-7	1.267E-7	2.353E-7
10	4.988E-7	8.826E-7	5.836E-7	1.031E-6
15	5.620E-7	9.913E-7	9.979E-7	1.777E-6
20	1.516E-6	2.681E-6	2.394E-7	4.187E-7
25	3.838E-7	6.711E-7	1.879E-6	3.324E-6
30	1.990E-6	3.464E-6	1.318E-6	2.152E-6
FPSS method				
5	8.980E-6	1.590E-5	3.165E-6	5.884E-6
10	1.244E-5	2.206E-5	1.456E-5	2.577E-5
15	1.402E-5	2.478E-5	2.489E-5	4.442E-5
20	3.782E-5	6.704E-5	5.958E-6	1.046E-5
25	9.360E-6	1.677E-5	4.673E-5	8.311E-5
30	4.889E-5	8.660E-5	3.011E-5	5.347E-5

preserve energy and charge very well. The discrete energy and charge conservation laws are preserved to an accuracy of 10^{-12} and 10^{-14}, respectively. Numerical results verify theoretical analysis.

Example 5.3. Consider the 2D-LS equation (1.8) with the long range potential $v(x,y)=1/\sqrt{x^2+y^2}$, and the laser field profile $\varepsilon(t)=\varepsilon_0 f(t)\cos(\omega t)$, where ε_0 is the peak amplitude of the laser field, ω is the frequency, $2\pi/\omega$ is the optical period of the laser field, and $f(t)$ describes the temporal shape of the pulse,

$$f(t)=\begin{cases}\sin\left(\dfrac{\pi}{2}\cdot\dfrac{t}{T_0}\right), & 0<t\leq T_0,\\ 1, & t>T_0.\end{cases} \tag{5.1}$$

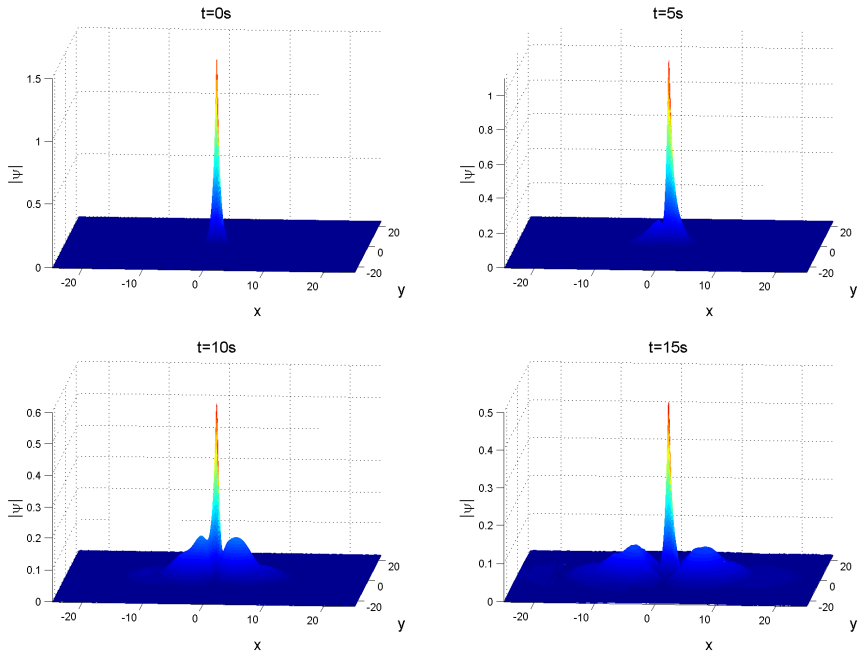

Figure 6: The laser-atom interaction for Example 5.3 by WCS method ($\tau=0.001$, $\Delta x=\Delta y=0.0625$).

Here, we choose parameters $\omega=2$, $\varepsilon_0=1$, $T_0=4$. The laser intensity is large enough for the electron to go through the potential barrier and be ionized. The initial condition is set to be the following ground state wave function

$$\psi(x,y,0)=2\sqrt{\frac{2}{\pi}}\cdot e^{-2\sqrt{x^2+y^2}}. \tag{5.2}$$

We solve the problem in spatial interval $[-25,25]\times[-25,25]$ till time $t=15$. The results of WCS and FPSS are similar. Therefore, we only show the results of WCS in Fig. 6. It can be seen that the electron is ionized and spread widely. We also can observe that both of the electron motion inside the atom and the ejected electron in the continuum. Meanwhile, the two methods are stable to simulate the laser-atom interaction when t becomes larger. The results indicate that WCS and FPSS for solving 2D-LS equation in quantum physics are efficient during long time computations.

6 Conclusions

In this paper, a wavelet collocation splitting method is constructed for solving 1D and 2D Schrödinger equations with variable coefficients. It is proved that the charge can be preserved exactly, and the global energy and momentum conservation laws can be preserved under several conditions, which make sure that proposed algorithms can preserve

the intrinsic properties of original problems as much as possible. Without consideration of symplectic, multi-symplectic or other conservation formulations for partial differential equations, the processes of proposed algorithms seem to be concise and much easier to implement for other cases. By the theoretical analysis and numerical experiments in comparison, WCS is an efficient and high accuracy method, and has conservative properties for 1D and 2D Schrödinger equations with variable coefficients during long time computations. The proposed methods can be naturally generalized to solve other complex cases or higher space dimensional equations.

Acknowledgments

The authors are very grateful to Prof. Weinan E for his encouragements and Dr. Huajun Zhu for comments on the present work. This work was supported by the National Natural Science Foundation of China (Grant Nos. 91130013, 10971226, and 11001270), Hunan Provincial Innovation Foundation (Grant Nos. CX2011B011, and CX2012B010), the Innovation Fund of NUDT (Grant No. B120205), and Chinese Scholarship Council.

References

[1] E. Infeldm, Nonlinear Waves: From Hydrodynamics to Plasma Theory, Advances in Nonlinear Waves, Pitman, Boston, 1984.
[2] C. Nore, A. Abid and M. Brachet, Small-Scale Structures in Three-dimensional Hydrodynamics and Magnetohyrodynamic Turbulence, Springer, Berlin, 1996.
[3] G.P. Agrawal, Nonlinear Fiber Optics, 3rd ed., Academic Press, San Diego, 2001.
[4] C. Sulem and P.L. Sulem, The Nonlinear Schrödinger equation: Self-focusing and Wave Collapse, Springer, New York,1999.
[5] W. Bao, D. Jaksch and P.A. Markowich, Numerical solution of the Gross-Pitaevskii equation for Bose-Einstein condensation, J. Comput. Phys. 187 (2003), 318-342.
[6] L. Stenflo and M.Y. Yu, Nonlinear wave modulation in a cylindrical plasma, IEEE Trans. Plasma Sci. 25 (1997), 1155-1157.
[7] W. Bao and J. Shen, A fourth-order time-splitting Lagurre-Hermite pseudo-spectral method for Bose-Einstein condensates, SIAM. Sci. Comput. 26 (2005), 2010-2028.
[8] D.G. Lappas and A. L'Huillier, Generation of attosecond XUV pulses in strong laser-atom interactions, Phys. Rev. A 58 (1998), 4140-4146.
[9] X.X. Zhou and C.D. Lin, Linear-least-squares fitting method for the solution of the time-dependent Schrödinger equation: Applications to atoms in intense laser fields, Phys. Rev. A 61 (2000) 053411.
[10] X.S. Liu, Y.Y. Qi, J.F. He and P.Z. Ding, Recent progress in symplectic algorithms for use in quantum system, Commun. Comput. Phys. 2 (2007), 1-53.
[11] Y.C. Fung, Biodynamics: Circulation, Springer-Verlag, New York, 1981.
[12] B. Tian, Y. Gao and H. Zhu, Variable-coefficient higher-order nonlinear Schrödinger model in optical fibers: Variable-coefficient bilinear form, Bäcklund transformation, brightons and symbolic computation, Phys. Lett. A 366 (2007), 223-229.

[13] V.N. Serkin and A. Hasegawa, Novel soliton solutions of the nonlinear Schrödinger equation model, Phys. Rev. Lett. 85 (2000), 4502-4505.
[14] H.J. Zhu, Y.M. Chen, S.H. Song and H.Y. Hu, Symplectic and multi-symplectic wavelet collocation methods for two-dimensional Schrödinger equations, Appl. Numer. Math. 61 (2011), 308-321.
[15] M. Delfour, M. Fortin and G. Payre, Finite-difference solutions of a nonlinear Schrödinger equation, J. Comput. Phys. 44 (1981), 277-288.
[16] Q.J. Meng, L.P. Yin, X.Q. Jin and F.L. Qiao, Numerical solutions of coupled nonlinear Schrödinger equations by orthogonal spline collocation method, Commun. Comput. Phys., 12 (2012), 1392-1416.
[17] Q.S. Chang, E.H. Jia and W. Sun, Difference schemes for solving the generalized nonlinear Schrödinger equation, J. Comput. Phys. 148 (1999), 397-415.
[18] S. Xie, G. Li and S. Yi, Compact finite difference schemes with high accuracy for one-dimensional nonlinear Schrödinger equation, Comput. Methods Appl. Mech. Engrg. 198 (2009), 1052-1060.
[19] M. Dehghan and A. Taleei, A compact split-step finite difference method for solving the nonlinear Schrödinger equations with constant and variable coefficients, Comput. Phys. Commun. 181 (2010), 43-51.
[20] J.B. Chen, M.Z. Qin and Y.F. Tang, Symplectic and multi-symplectic methods for the nonlinear Schrödinger equation, Comput. Math. Appl. 43 (2002), 1095-1106.
[21] J.B. Chen, A multisymplectic integrator for the periodic nonlinear Schrödinger equation, Appl. Math. Comput. 170 (2005), 1394-1417.
[22] J.L. Hong and L.H. Kong, Novel multi-symplectic integrators for nonlinear fourth-order Schrödinger equation with trapped term, Commun. Comput. Phys. 7 (2010), 613-630.
[23] Y.M. Chen, H.J. Zhu and S.H. Song, Multi-symplectic splitting method for the coupled nonlinear Schrödinger equation, Comput. Phys. Commun. 181 (2010), 1231-1241.
[24] X. Qian, Y.M. Chen, E. Gao and S.H. Song, Multi-symplectic wavelet splitting method for the strongly coupled Schrödinger system, Chin. Phys. B 21 (2012), 120202.
[25] J.X. Cai, Y.S. Wang and H. Liang, Local energy-preserving and momentum-preserving algorithms for coupled nonlinear Schrödinger system, J. Comput. Phys. 239 (2013), 30-50.
[26] J.L. Hong, Y. Liu, H. Munthe-Kaas and A. Zanna, Globally conservative properties and error estimation of a multi-symplectic scheme for Schrödinger equations with variable coefficients, Appl. Numer. Math. 56 (2006), 814-843.
[27] M.J. Gotay, A multisymplectic framework for classical field theory and the calculus of variations. I: Covariant Hamiltonian formalism, M. Francaviglia (ed.), Mechanics, analysis and geometry: 200 years after Lagrange. Amsterdam etc.: North-Holland (1991), 203-235.
[28] S. Kouranbaeva and S. Shkoller, A variational approach to second-order multiisymplectic field theory, J. Geom. Phys. 35 (2000), 333-366.
[29] J.L. Hong and Y.J. Sun, Generating functions of multi-symplectic RK methods via DW Hamilton-Jacobi equations, Numer. Math. 110 (2008), 491-519.
[30] H.J. Zhu, L.Y. Tang, S.H. Song, Y.F. Tang and D.S. Wang, Symplectic wavelet collocation method for Hamiltonian wave equations, J. Comput. Phys. 229 (2010), 2550-2572.
[31] G. Strang, On the construction and comparison of difference scheme, SIAM J. Numer. Anal. 5 (1968), 506-517.
[32] H.Q. Wang, Numerical studies on the split-step finite difference method for nonlinear Schrödinger equations, Appl. Math. Comput. 170 (2005), 17-35.
[33] H.J. Zhu, S.H. Song and Y.F Tang, Multi-symplectic wavelet collocation method for the non-

linear Schrödinger equation and the Camassa-Holm equation, Comput. Phys. Commun. 182 (2011), 616-627.

[34] S. Bertoluzza and G. Naldi, A wavelet collocation method for the numerical solution of partial differential equations, Appl. Comput. Harm. Anal. 3 (1996), 1-9.

[35] Y.L. Zhou, Application of Discrete Functional Analysis to the Finite Difference Method, International Academic Press, Hong Kong, 1990.

[36] X. Qian, S.H. Song, E. Gao and W.B. Li, Explicit multi-symplectic method for the Zakharov-Kuznetsov equation, Chin. Phys. B 21 (2012), 070206.